

RL-TR-95-280
In-House Report
January 1996



DEMONSTRATION OF HIGH DISPERSIVE FIBER BASED OPTICAL PROCESSOR

Steven T. Johns
Douglas A. Norton

APPROVED FOR PUBLIC RELEASE; DISTRIBUTION UNLIMITED.

Rome Laboratory
Air Force Materiel Command
Rome, New York

19960311 208

DTIC QUALITY INSPECTED 1

This report has been reviewed by the Rome Laboratory Public Affairs Office (PA) and is releasable to the National Technical Information Service (NTIS). At NTIS, it will be releasable to the general public, including foreign nations.

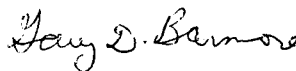
RL-TR-95- 280 has been reviewed and is approved for publication.

APPROVED:



JAMES W. CUSACK, Chief
Photonics Division
Surveillance and Photonics Directorate

FOR THE COMMANDER:



GARY D. BARMORE, Major, USAF
Deputy Director
Surveillance and Photonics Directorate

If your address has changed or if you wish to be removed from the Rome Laboratory mailing list, or if the addressee is no longer employed by your organization, please notify Rome Laboratory/ (OCPA), Rome NY 13441. This will assist us in maintaining a current mailing list.

Do not return copies of this report unless contractual obligations or notices on a specific document require that it be returned.

REPORT DOCUMENTATION PAGE

Form Approved
OMB No. 0704-0188

Public reporting burden for this collection of information is estimated to average 1 hour per response, including the time for reviewing instructions, searching existing data sources, gathering and maintaining the data needed, and completing and reviewing the collection of information. Send comments regarding this burden estimate or any other aspect of this collection of information, including suggestions for reducing this burden, to Washington Headquarters Services, Directorate for Information Operations and Reports, 1215 Jefferson Davis Highway, Suite 1204, Arlington, VA 22202-4302, and to the Office of Management and Budget, Paperwork Reduction Project (0704-0188), Washington, DC 20503.

1. AGENCY USE ONLY (Leave Blank)		2. REPORT DATE January 1996	3. REPORT TYPE AND DATES COVERED In-House Oct 93 - Sep 95	
4. TITLE AND SUBTITLE DEMONSTRATION OF HIGH DISPERSIVE FIBER BASED OPTICAL PROCESSOR			5. FUNDING NUMBERS PR - 4600 TA - P1 WU - 16	
6. AUTHOR(S) Steven T. Johns, Douglas A. Norton			8. PERFORMING ORGANIZATION REPORT NUMBER RL-TR-95-280	
7. PERFORMING ORGANIZATION NAME(S) AND ADDRESS(ES) Rome Laboratory (OCPA) 25 Electronic Pky Rome, NY 13441-4515			10. SPONSORING/MONITORING AGENCY REPORT NUMBER N/A	
9. SPONSORING/MONITORING AGENCY NAME(S) AND ADDRESS(ES) Rome Laboratory (OCPA) 25 Electronic Pky Rome, NY 13441-4515			11. SUPPLEMENTARY NOTES Rome Laboratory Project Engineer: Steven T. Johns/OCPA (315)330-4456	
12a. DISTRIBUTION/AVAILABILITY STATEMENT Approved for public release, distribution unlimited.			12b. DISTRIBUTION CODE	
13. ABSTRACT (Maximum 200 words) We have demonstrated a tapped delay line microwave filter based on the use of high dispersion fiber as the tunable time delay. This system offers advantages of high bandwidth and tunability over current methods of time delay filtering. The method uses a single length of high dispersion fiber to achieve a variable time delay. By tuning the wavelength the relative time delay is changed. For a 1 km length of high dispersion fiber (-98 ps/km-nm) approximately 5ns of delay has been demonstrated over a 50 nm tuning range.				
14. SUBJECT TERMS optical signal processing, high dispersion fiber optics, true time delay, microwave optics			15. NUMBER OF PAGES 50	
			16. PRICE CODE	
17. SECURITY CLASSIFICATION OF REPORT UNCLASSIFIED	18. SECURITY CLASSIFICATION OF THIS PAGE UNCLASSIFIED	19. SECURITY CLASSIFICATION OF ABSTRACT UNCLASSIFIED	20. LIMITATION OF ABSTRACT U/L	

Table of Contents

1.0	Introduction.....	1
2.0	Dispersion Measurements.....	3
2.1	Fiber Characteristics.....	3
2.2	RF Bandwidth Performance.....	5
3.0	True Time Delay	6
3.1	Pulse Propagation Delay Measurements	6
4.0	Delay Line Filtering Using High Dispersive Optical Fiber.....	8
4.1	Transversal Filters	8
4.2	Optical Transversal Filtering.....	8
4.3	Fiber Transversal Filter Concept.....	9
4.3.1	Optical Filtering Experiment Layout.....	10
4.3.2	Experimental Results	10
5.0	Summary.....	13

List Of Figures

2.1	True Time Delay Experiment Set-up.....	14
2.2	Phase Response for a Narrow Band of Optical Carriers.....	15
2.3	Phase Response for a 50+nm Band of Optical Carriers.....	16
2.4	Dispersion vs. Wavelength.....	17
2.5	Delay vs. Wavelength.....	18
3.1	Basic Time Delay Architecture	19
3.2	True Time Delay Experiment Set-up.....	20
3.3	Optical Spectrum of Laser Diodes	21
3.4	Electrical Pulse Width.....	22
3.5	Optical Pulses Prior to High Dispersion Fiber	23
3.6	Impulse Response of Two Tap System.....	24
3.7	Frequency Response of Two Tap System.....	25
4.1	Transversal Filter	26
4.2	Idealized Optical Transversal Filter	27
4.3	8 Channel Transversal Filter.....	28
4.4	Laser Diode Spectrum with 0.87 nm Wavelength Spacing.....	29
4.5	Measured Frequency Response for 0.87 nm Wavelength Spacing.....	30
4.6	Calculated Frequency Response for 0.87 nm Wavelength Spacing	31
4.7	Laser Diode Spectrum with 1.24 nm Wavelength Spacing.....	32
4.8	Measured Frequency Response for 1.24 nm Wavelength Spacing.....	33
4.9	Calculated Frequency Response for 1.24 nm Wavelength Spacing	34

List of Appendix

Appendix A..... 36
Appendix B..... 38

1.0 Introduction

Fiber based delay lines have been a suggested method of time delay for several years. Fiber delay lines offer large bandwidths and wide dynamic range, all in a small package size. Several different methods have been demonstrated using fiber delay lines, most of which use several fixed lengths of fiber to achieve stepped time delay.

A concept proposed by Soref [1, 2] indicates that time delay steering is readily available from a high-dispersion fiber-optic feed by wavelength-tunable laser diode source. The method which we employ exploits that high dispersion to achieve a variable time delay. By tuning the wavelength the relative time delay is changed.

Corning Incorporated (Corning NY) has developed a new high dispersion single mode fiber with negative chromatic dispersion intended to compensate for or cancel the positive dispersion found in standard telecommunication fiber [3]. This new single mode optical fiber has a segmented core and a propagation loss of 1 dB/km at 1550 nm wavelength [3]. The advantage of this fiber is that its dispersion of -98 ps/nm-km is 5.4 times larger than that of the standard single mode fiber at +18 ps/nm-km. This is the fiber which was used throughout our measurements and referred to in this report.

This report will document the use of high dispersion fiber in an optical tapped delay line filter. In the second chapter, we will describe the measurement of fiber dispersion and most importantly the minimal group delay across the RF bandwidth of interest. In the third chapter, we demonstrate the actual delay of a pulse carried on two different optical carriers. These optical carriers are of different wavelength and therefore have different transit times in the high dispersion fiber. In the fourth chapter, we describe calculated and measured filter responses of our 8 tap transversal filter experiment. The fifth chapter discusses

several applications which could benefit from the use of this technology. And finally, the sixth chapter summarizes the results of this project.

2.0 Dispersion Measurement

Before this high dispersion fiber can be used in an RF application and in particular an RF application which is considered wide band, the fiber must be measured for dispersion.

This measurement of fiber dispersion will allow us to make an estimate of the group velocity across the RF bandwidth. We are suggesting that the use of this fiber is more appropriate for ultra wideband applications starting with 500 MHz up to 5 GHz, particularly in our application which is discussed in Chapter 4. Therefore it is important to know the effect this dispersion will have on this large bandwidth.

2.1 Fiber Characterization

The system which provides this variable true time delay is illustrated in Fig 2.1. An RF signal is applied to the external modulator that amplitude modulates the light beam from a variable-wavelength laser. The light is sent into the high dispersion fiber and is demodulated at the far end of the fiber. A photodiode at the far end is equally sensitive to all input wavelengths. Depending on the optical input wavelength, the time to traverse the fiber will be different due to the chromatic dispersion (D) of the fiber. Thus, in this scheme, the incremental (programmable) time delay would be proportional to $\Delta\lambda$ the change in laser wavelength, where L is the length of the fiber.

$$\Delta\tau = DL\Delta\lambda$$

The 1 km of high dispersion fiber used has a total loss of 2 dB at 1550 nm, where 1 dB is due to the fiber and 1 dB is due to the coupling loss of the splices. The pigtailed laser source was a Photonetics Tunics 1550I wavelength tunable external cavity InGaAs laser

diode [4]. This laser has a 100 KHz linewidth and is continuously tunable between 1500 nm and 1560 nm. The optical signal was then modulated between 100 MHz and 3 GHz with a Crystal Technology 2 x 2 LiNbO₃ electro-optic switch used as an amplitude modulator. A GTE 25 m Er³⁺ fiber amplifier compensated for the optical signal loss due to the switch. The optical carrier then traversed the 1km of high dispersion fiber, attenuator and finally was detected by a photodetector. An HP 8753C network analyzer was used both as a RF source to drive the modulator and to measure the RF signal from the photodiode.

A calibration of the measurement system consisting of all of the above components except for the device under test (DUT), was performed on the network analyzer using 1601 samples over the 2.9 GHz bandwidth, no averaging or smoothing was used for any of these tests.

With the DUT in the system, a reference wavelength of 1525 nm was selected and then the laser wavelength was varied and the change in RF phase was measured. Figure 2.2 and Figure 2.3 shows the change in phase over the 2.9 GHz bandwidth for several different optical wavelengths. The increase in noise at the lower wavelengths (1523 nm) is due to the drop off in gain in the Er³⁺ fiber amplifier. Our setup allowed direct measurement of the wavelength dependence of fiber dispersion. That result is given in Figure 2.4. Also a relative time delay of 4.66 ns for 47 nm change in laser diode wavelength was measured and shown in Figure 2.5. The observed programmable delay was quite linear in laser wavelength.

2.2 RF Bandwidth Performance

We can show that the high dispersion of this fiber, -98 ps/nm-km, does not introduce much distortion to the microwave signal, and does not cause significant optical pulse broadening. Over an RF bandwidth of B, the difference in time delay caused by the fiber dispersion is given by

$$\Delta t = DL \left[\lambda^2 \frac{B}{C} \right].$$

For a typical phased array, B = 2 GHz propagated through L = 1 km of this high dispersion fiber, with $\lambda=1550$ nm, we find that $\Delta\tau = 1.5$ ps. Therefore, the dispersive delay has little effect in diminishing good microwave performance. In other words, true time delay is seen across the RF bandwidth. This shows not only the utility of this optical delay for phased arrays, but also proves that the same method of time delay is useful for other RF processing, such as tunable optical transversal filtering, recirculating delay lines, and parallel-to-serial data multiplexers.

The 5 ns of variable delay measured in the project is quite applicable to an NxN element phased array. For example, if the element spacing is $\lambda_{RF}/2$ and the maximum scan angle θ , then the maximum required incremental time delay is $\Delta\tau_{max} = N \sin \theta / (2f_{RF})$. We find that $\Delta\tau_{max} = 5$ ns for $\theta = 90^\circ$ and N = 50 and $f_{RF} = 5$ GHz. The minimum required incremental time delay in a typical phased array is approximately (1/100) $\Delta\tau_{max}$, so the smallest required delay step is ~ 0.05 ns in this example. For future implementations of dispersive delay, we note that AT&T Bell Labs is currently developing a laser diode that is tunable over 57 nm with a few nanosecond wavelength reconfiguration time [5]. The related time delay work by Esman *et al.* [7] used a +18 ps/nm-km fiber and a bench top fiber ring laser with a Faraday mirror and electrically tuned Fabry-Perot filter instead of a semiconductor diode source.

3.0 True Time Delay

3.1 Pulse Propagation Delay Measurements

The configuration of a high dispersion time delay system is shown in Figure 3.1. The basic time delay system is comprised of a tunable laser diode, an RF modulator, high dispersion fiber, and detector. If the laser diode can be directly modulated, this system is further simplified. The change in time delay produced by such a system was shown to be linear over a wavelength spectrum of 50 nm.

An excellent way to demonstrate the true time delay nature of this system is to propagate a pulse down the high dispersive fiber. This pulse is carried by two optical wavelengths. The two wavelengths can also be used to measure the impulse response and transfer function of a two tap delay line filter. The layout of this two tap system is shown in Figure 3.2. It is based on the layout in Figure 3.1 in which a second laser source has been added.

This system is comprised of two pig-tailed DFB lasers, $\lambda_1 = 1527$ nm and $\lambda_2 = 1540$ nm; each source passes through an optical attenuator and polarization controller. The optical spectrum of the laser diodes is shown in Figure 3.3. The attenuators are used to both balance and unbalance the filter through optical amplitude weighting. The fibers are combined using a 2x2 fiber coupler and then the composite optical signal is amplitude modulated with a 2x2 LiNbO₃ electro-optic switch. The RF modulated light passes through 1km of high dispersion fiber and is then detected. Because of the difference in wavelength, the two optical carriers will be delayed with respect to each other by the amount:

$$\Delta t = \Delta\lambda DL$$

where $\Delta\lambda = 13$ nm, $D = -98$ ps/nm-km and $L = 1$ km.

A single 0.5 ns pulse was applied to the 2x2 electro-optical switch, shown in Figure 3.4. A measurement of the rise and fall times of the optical pulse created by the modulator shows some broadening and a small tail, shown in Figure 3.5. The broadening and tail are due to the frequency response of the optical detector. The dispersion in the high dispersion fiber caused a pulse separation of 1.3 ns. The impulse response is shown in Figure 3.6 for this system. The dispersion fiber's effect on group delay is minimal. [9] Over an RF bandwidth of B , the change in time delay caused by the fiber dispersion is

$$\Delta t = DL[\lambda^2 B/c].$$

If the 0.5 ns pulse is taken to have a bandwidth of $B = 2$ GHz and $\lambda = 1550$ nm, the maximum change in delay across this bandwidth is 1.5 ps. This very small delay amounts to a change across the RF bandwidth of only a fraction of a pulse width.

Using a network analyzer, the filter's transfer function was measured by scanning the RF spectrum between 100 KHz and 3 GHz. The RF signal was applied to the 2x2 switch and the detector output was returned to the network analyzer for measurement. The 1.3 ns spacing of the two taps equates to a sampling frequency of 769 MHz. In agreement with theory, this two tap filter produced a 20 dB null at 396 MHz and 1188 MHz as shown in Figure 3.7.

4.0 Delay Line Filtering using High Dispersive Optical Fiber

The fact that changing the wavelength of light traveling through a high dispersive fiber will change its transit time leads to an implementation of a transversal filter. Using a single fiber for the several delay lines or channels, demonstrates not only the usefulness of high dispersive fiber, but also the benefit of the parallel nature of light.

4.1 Transversal Filters

Transversal filters or tapped delay line filters are realized by summing several delayed and weighted versions of the same waveform. In a more traditional sense, this is achieved using several different length transmission lines and some mechanism for variable weights. These weights are then summed together to create the filtering function. This is shown in Figure 4.1 and equates to

$$y(t) = \sum_k^N w_k x(t - k\tau)$$

As seen from this figure, the signal at each tap is weighted by the appropriate coefficient and the resulting products are summed to form the filtered output $y(t)$. The appropriate coefficient or weighting is determined from the impulse response corresponding to a desired filter function. This coefficient is considered to be bipolar in most conventional transversal filtering applications.

4.2 Optical Transversal Filtering

The use of optics in the area of microwave applications offers many attractive benefits and in the case of microwave transversal filtering this is especially true. Early efforts in

microwave optics demonstrated transversal filters which substituted various lengths of optical fiber for more traditional delay lines. This worked well by decreasing size and weight and increasing available bandwidth. But it did not exploit the parallel nature of light nor did it allow for quick delay reconfiguration. If the filter function required different delay lengths, new fiber lengths were needed to produce the different delays.

Our transversal filter, based on a single length of high dispersive fiber, does exhibit all the same qualities of earlier tapped delay lines but also can be reconfigured in real time. This results in a system which not only has a wide bandwidth, but is also adaptable to many processing applications. There are also applications which only now become practical using this technology, these applications will be described later in this report.

4.3 Fiber Transversal Filter Concept

In the most idealized case, a transversal filter using high dispersion optical fiber could be realized using a broadband source, optical modulator, high dispersion fiber, and detector. This idealized system is shown in Figure 4.2.

In this system, RF modulated broadband light would traverse the high dispersion fiber. Upon exiting this fiber, this band of light would be linearly delayed across its spectrum. Then using some device which could selectively weight various bands of the spectrum, the light could be summed in a detector to form the desired filter. This wavelength weighting device could be envisioned as a grating which would spread the spectrum into a band of colors where they would be weighted using a spatial light modulator (SLM).

In reality, it is difficult to find a continuous broadband source which can be modulated at a microwave frequency, therefore a comb of wavelengths was used. This comb of

wavelengths was created using eight laser diodes which were coupled into a single fiber. Each laser diode was current and temperature controlled to yield the desired weighting and system flexibility.

4.3.1 Optical Filtering Experiment Layout

The eight tap filter, shown in Figure 4.3, is comprised of eight pig-tailed Mitsubishi ML974A2f distributed feedback laser (DFB) diodes. These DFB lasers had room temperature output wavelengths that ranged from 1553 nm to 1561 nm. The lasers were then temperature tuned to produce the required wavelength characteristics necessary for the experiments. Each DFB laser had a polarization controller (specification shown in Appendix A) to maximize the transmitted optical power through the modulator. The individual fibers from each DFB laser are then combined using two 4 x 1 and a 2 x 1 Gould Fiber Couplers. With eight DFB lasers coupled to a single fiber, they were then sent into an AT&T external modulator to place the RF signal on the optical carrier. This modulator had a bandwidth of 4.8 GHz with an optical insertion loss of 3.3 dB. The optical signal was then launched into the 1 km length of high dispersion fiber and detected by a NewFocus 1514 6 GHz photoreceiver module and amplified by a NewFocus 1422 RF amplifier. An HP8753C network analyzer was used to both drive the external modulator and measure the detected RF signal.

4.3.2 Experiment Results

The network analyzer was used to measure the filter's transfer function by sweeping RF frequencies between 300 MHz and 6 GHz and measuring the response of the system. The network analyzer was calibrated to remove any amplitude changes across the RF bandwidth of the modulator and detector. This change in response was due to the bandwidth of these

two devices, the calibration has little affect on the results shown here. This calibration could have been replaced with a properly designed network.

In the system tested, laser diodes had a maximum wavelength spacing of about 1.25 nm, using a 1 km length of high dispersion fiber ($-98 \text{ ps}/(\text{km nm})$) this would result in an incremental time delay of 0.12 ns. Each laser or tap weight could be varied to 32 levels, if a more aggressive method for diode output stabilization was used the number of levels could be as high as 64 or greater.

For our experiment we wanted to demonstrate the reconfigurability of the system. This ability to reconfigure quickly sets this system apart from other optical transversal filters. This ability not only lends well to traditional filters but also systems which look for multiple distributed scatterers. Using our system, taps could be adjusted to look for particular scatterers. Only those scatterers having a sum above a certain threshold would be detected and identified.

In our experiments, the reconfigurability of the system was demonstrated by changing the wavelength spacing of the laser diodes. The spacing was uniform across the spectrum to demonstrate the system's response in terms which are familiar to most engineers. Two cases are shown here where the wavelength spacing is set to 0.87 nm and 1.24 nm. Figure 4.4 and Figure 4.7 show the wavelength spacing used. These wavelength spacings produced incremental time delays of 0.08 ns and 0.12 ns respectively.

Using Mathematica, we calculated the transfer function of the system using the same relative amplitudes and wavelength spacings of the laser diodes. The Mathematica code is included in Appendix B. The actual filter response was measured as described above. The measured response for 0.87 nm and 1.24 nm wavelength spacing is shown in Figure 4.5

and Figure 4.8 respectively. These show a sampling frequency of 12.5 GHz which produces an approximately 30 dB null at 1.4 GHz for 0.87 nm spacing. For the 1.24 nm spacing the filter produced a 22 dB null at 1.3 GHz. The calculated filter response, shown in Figure 4.6 and 4.7, shows good agreement with the measurements.

5.0 Summary

A new High Dispersion Optical Fiber designed by Corning Inc. has been tested in a true time delay system. The system produced 5 ns of programmable RF delay for a 50 nm tunable laser source. Additional experiments in which two laser diodes were used demonstrated that the high dispersion fiber can be utilized as a RF tapped delay line filter. Initial experiments with the two tap filter system produced a 20 dB null at 396 MHz and at 1188 MHz. In an effort to demonstrate scalability, an eight tap system was fabricated. A variable incremental time delay was produced by changing the wavelength spacing of the laser diodes. Incremental delays of 0.08 ns and 0.12 ns were produced with wavelength spacings of 0.87 nm and 1.24 nm. This eight tap system produced 30 dB null at 1.4 GHz and a 22 dB null at 1.3 GHz.

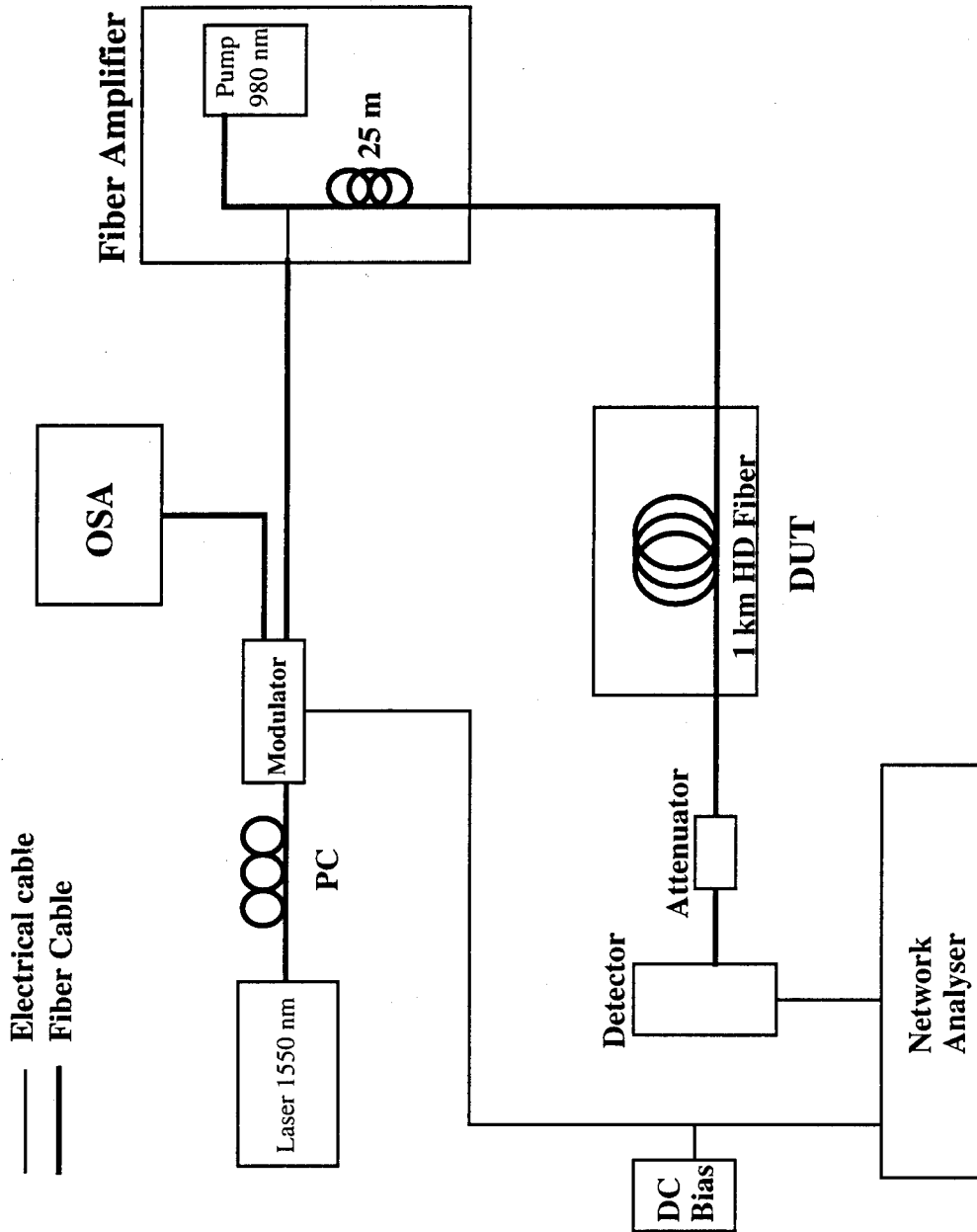
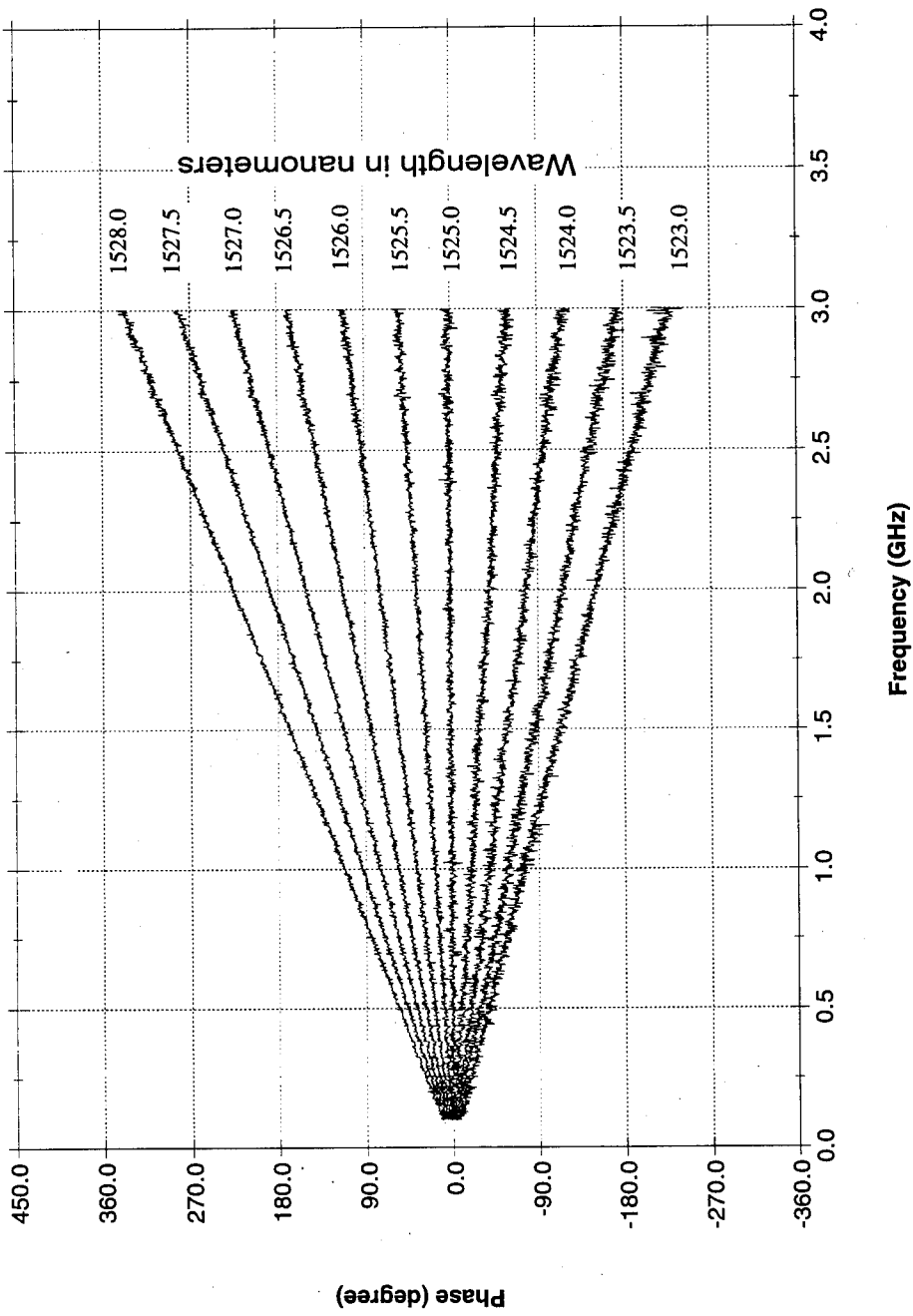
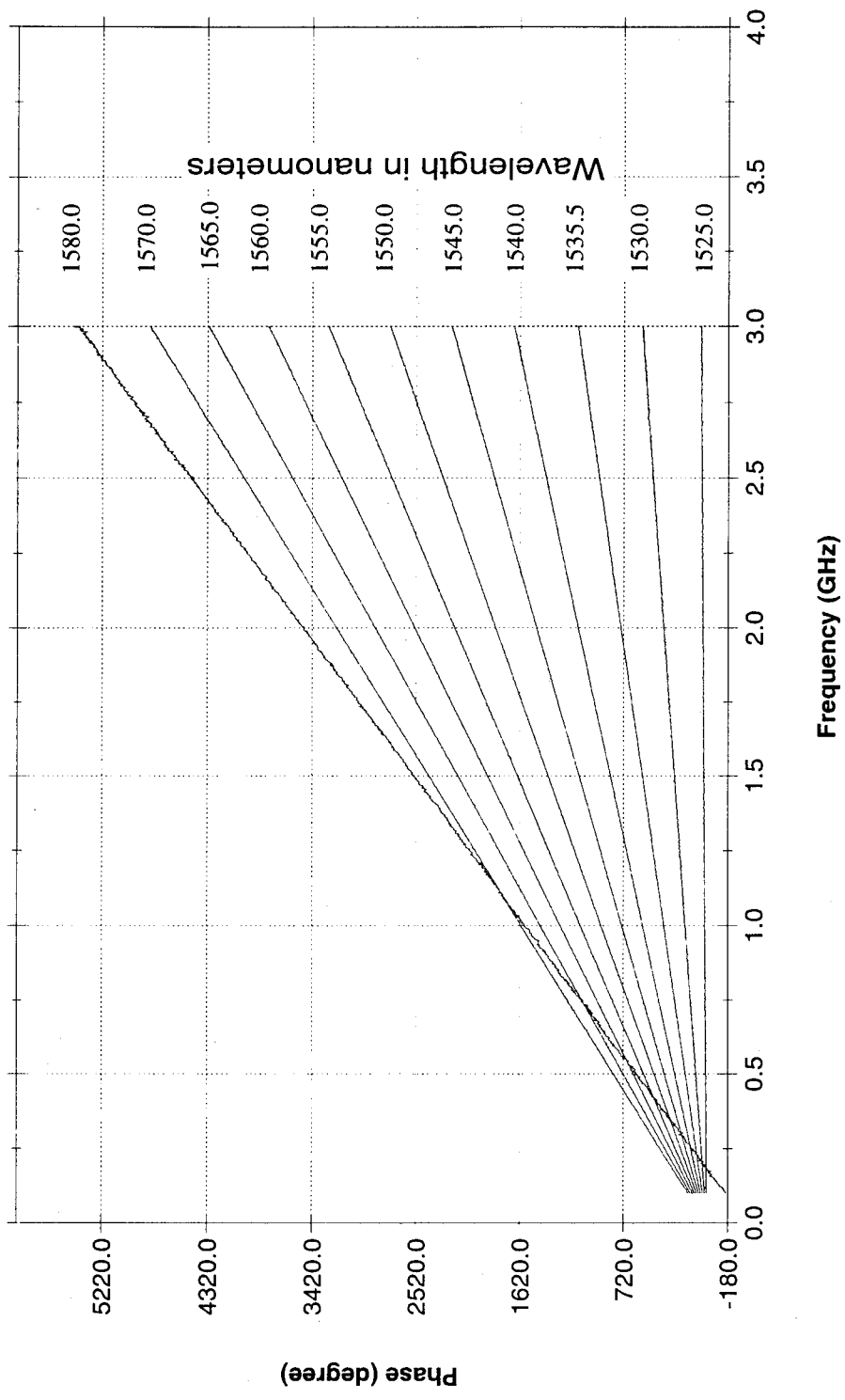


Figure 2.1 True Time Delay Experiment Set-up



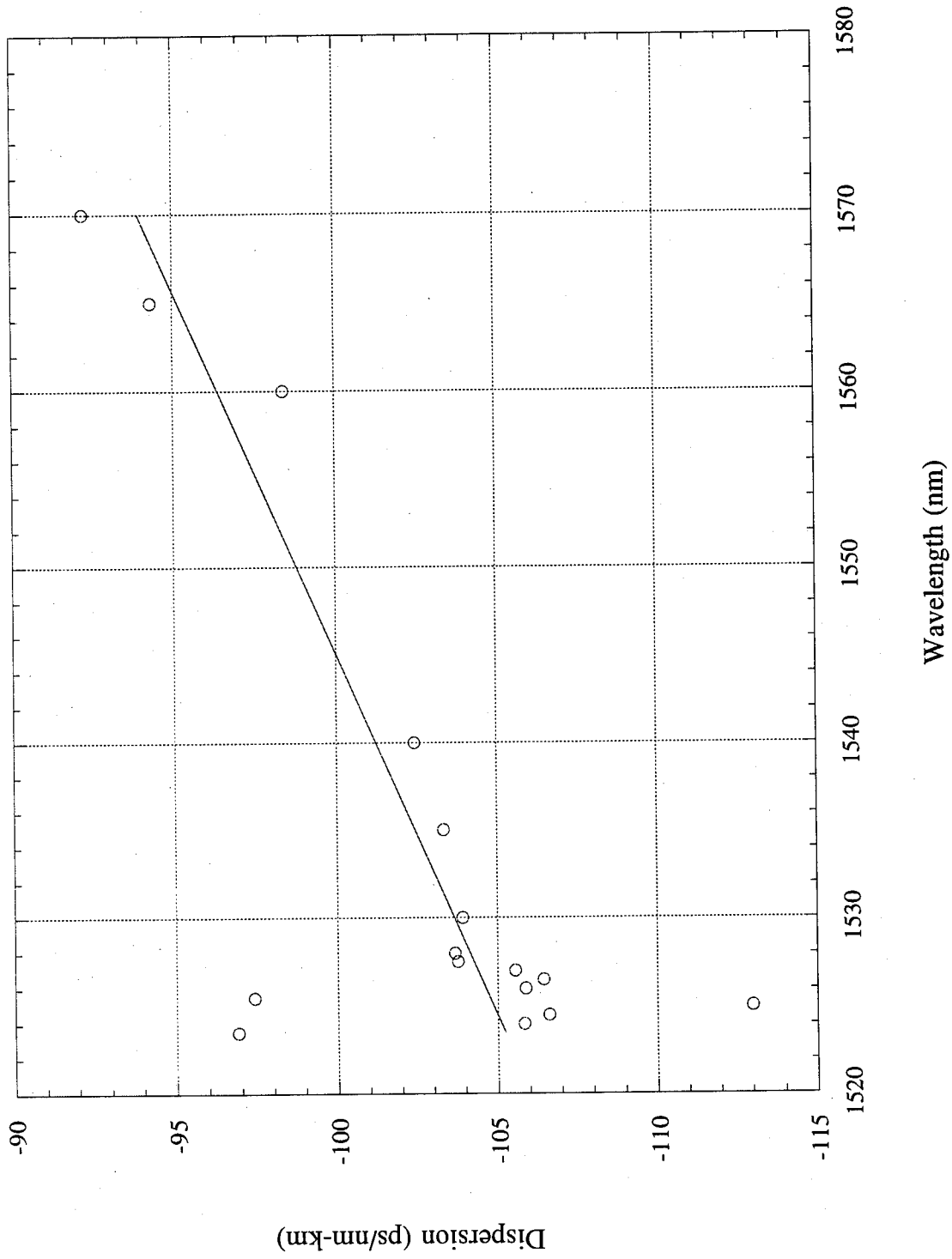
Phase Response for a Narrow Band of Optical Carriers

Figure 2.2

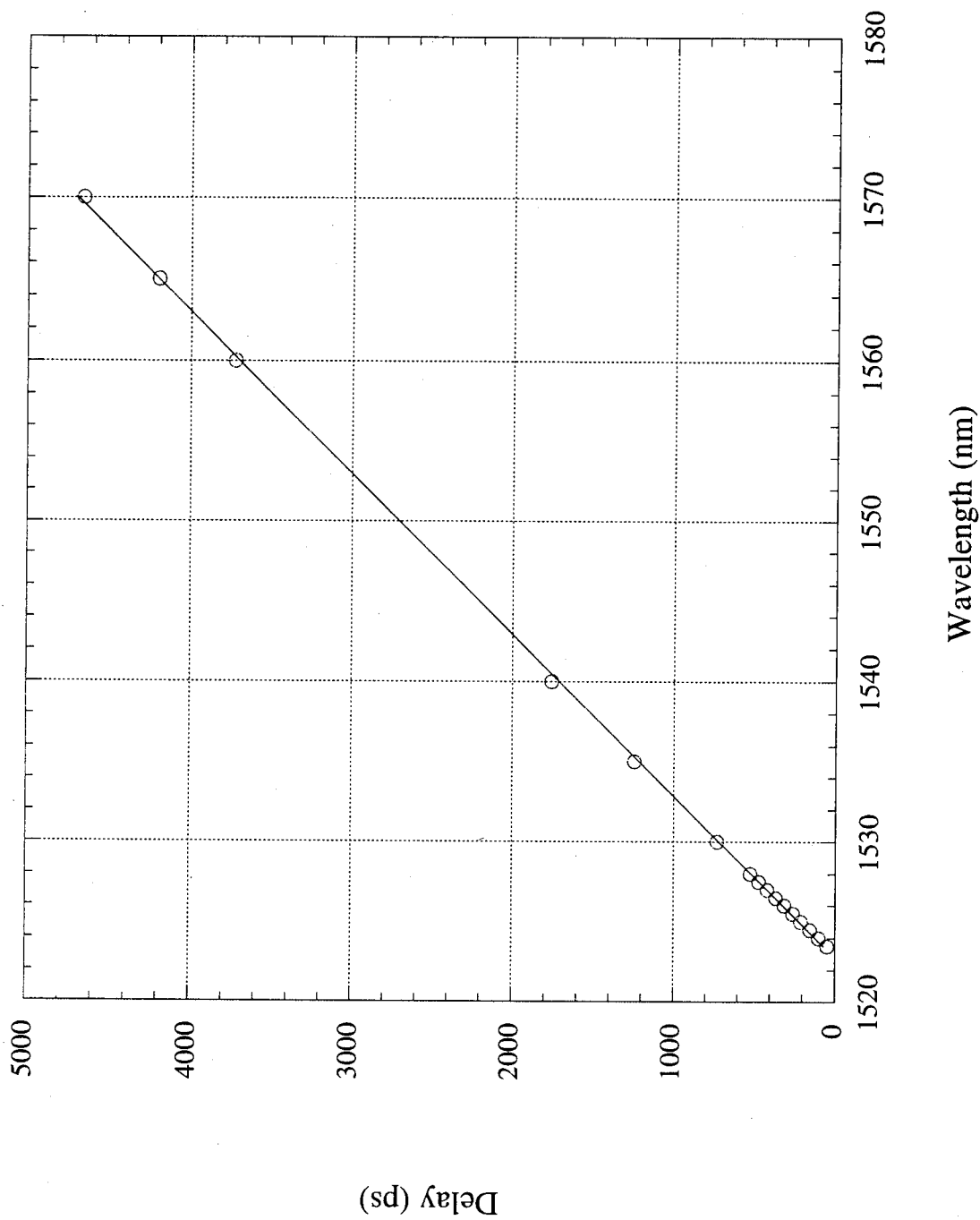


Phase Response for a 50+nm Band of Optical Carriers

Figure 2.3



Dispersion vs. Wavelength
Figure 2.4



**Delay vs. Wavelength
Figure 2.5**

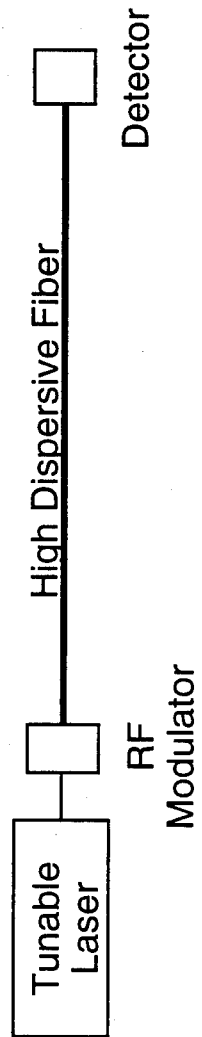
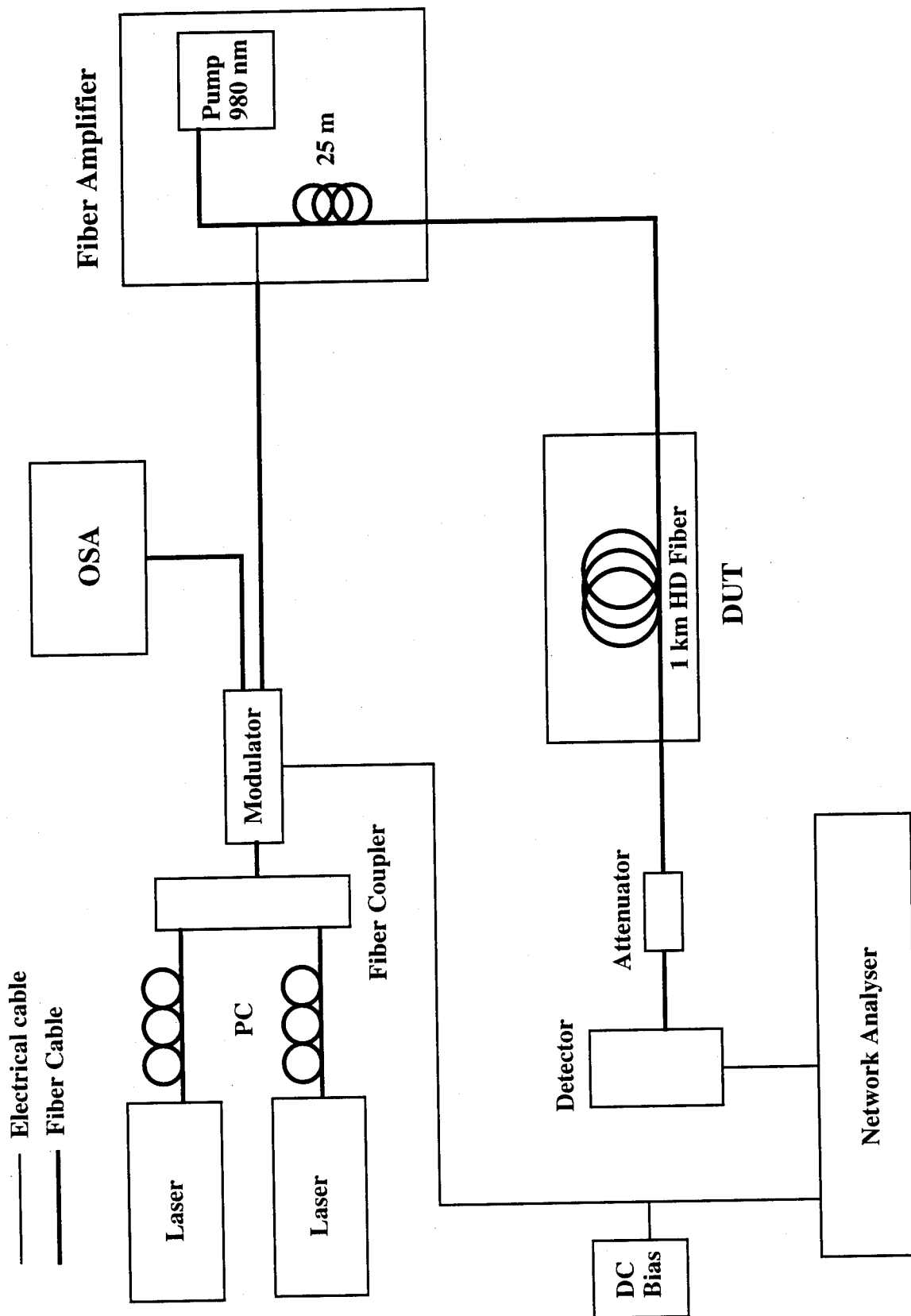


Figure 3.1 Basic Time Delay Architecture



True Time Delay Experiment Set-up
Figure 3.2

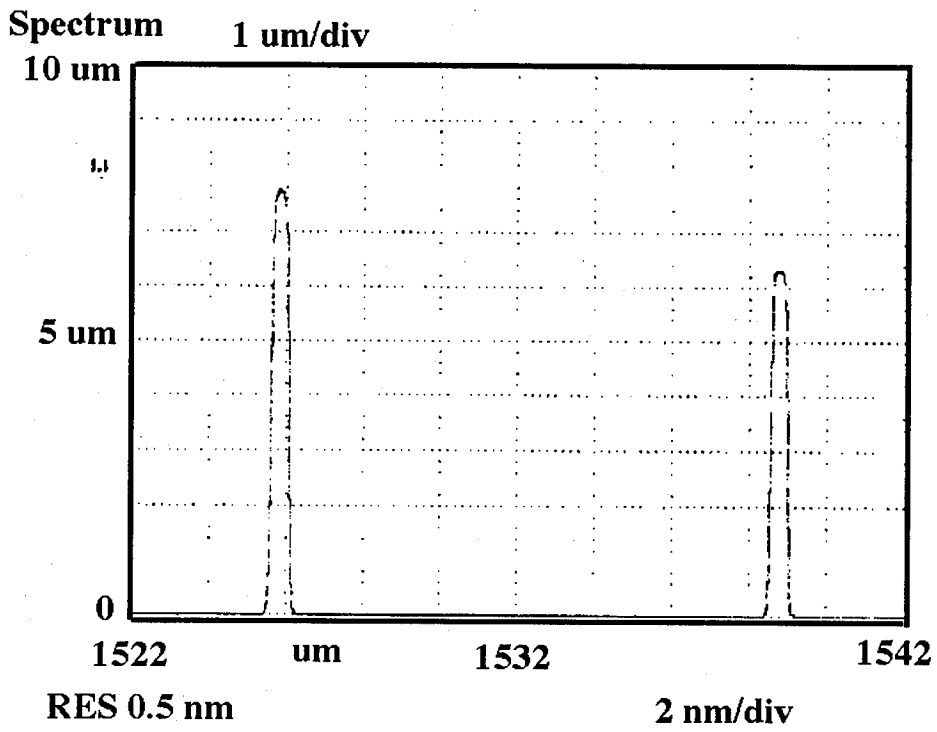


Figure 3.3 Optical Spectrum of Laser Diodes

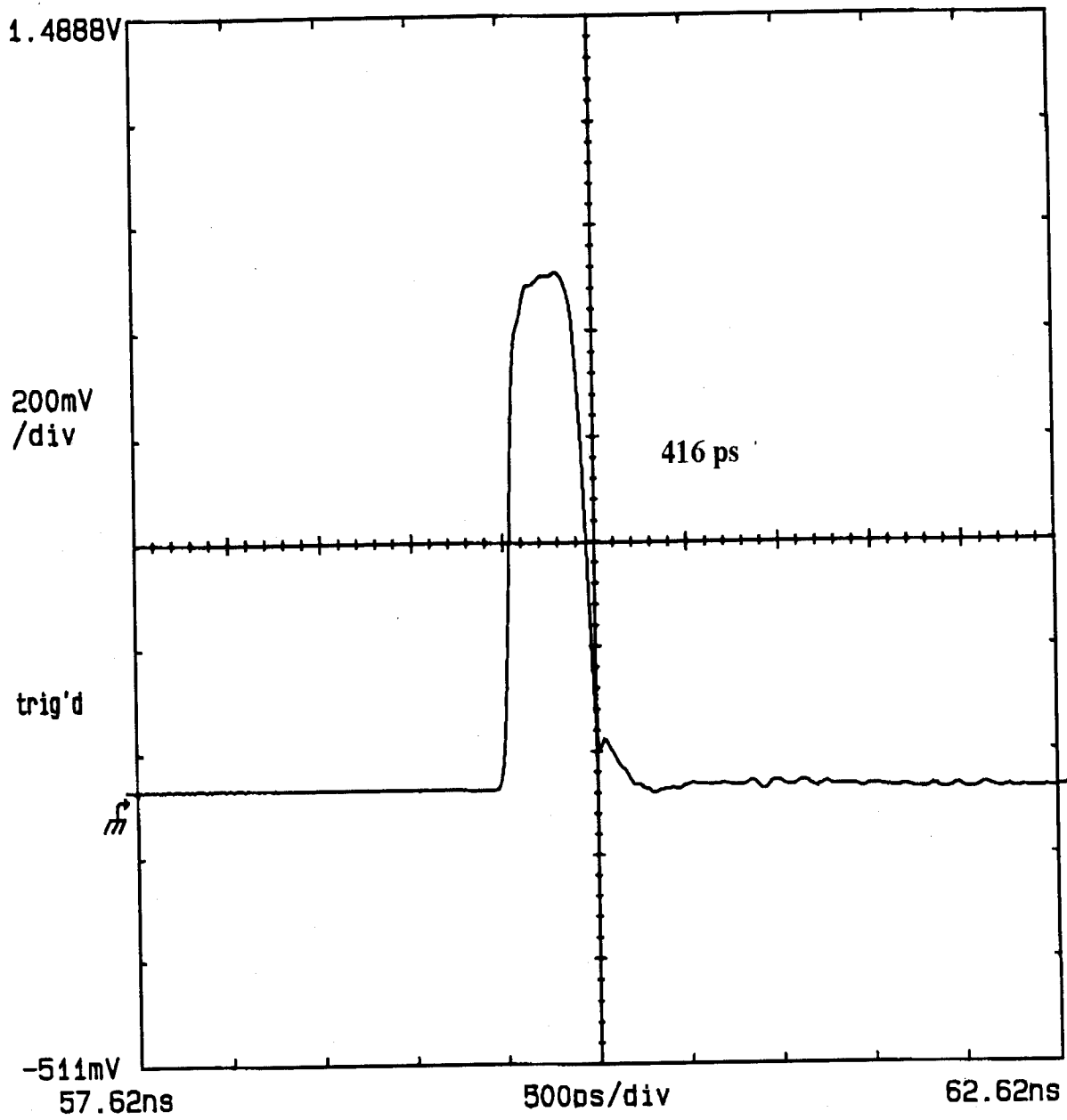
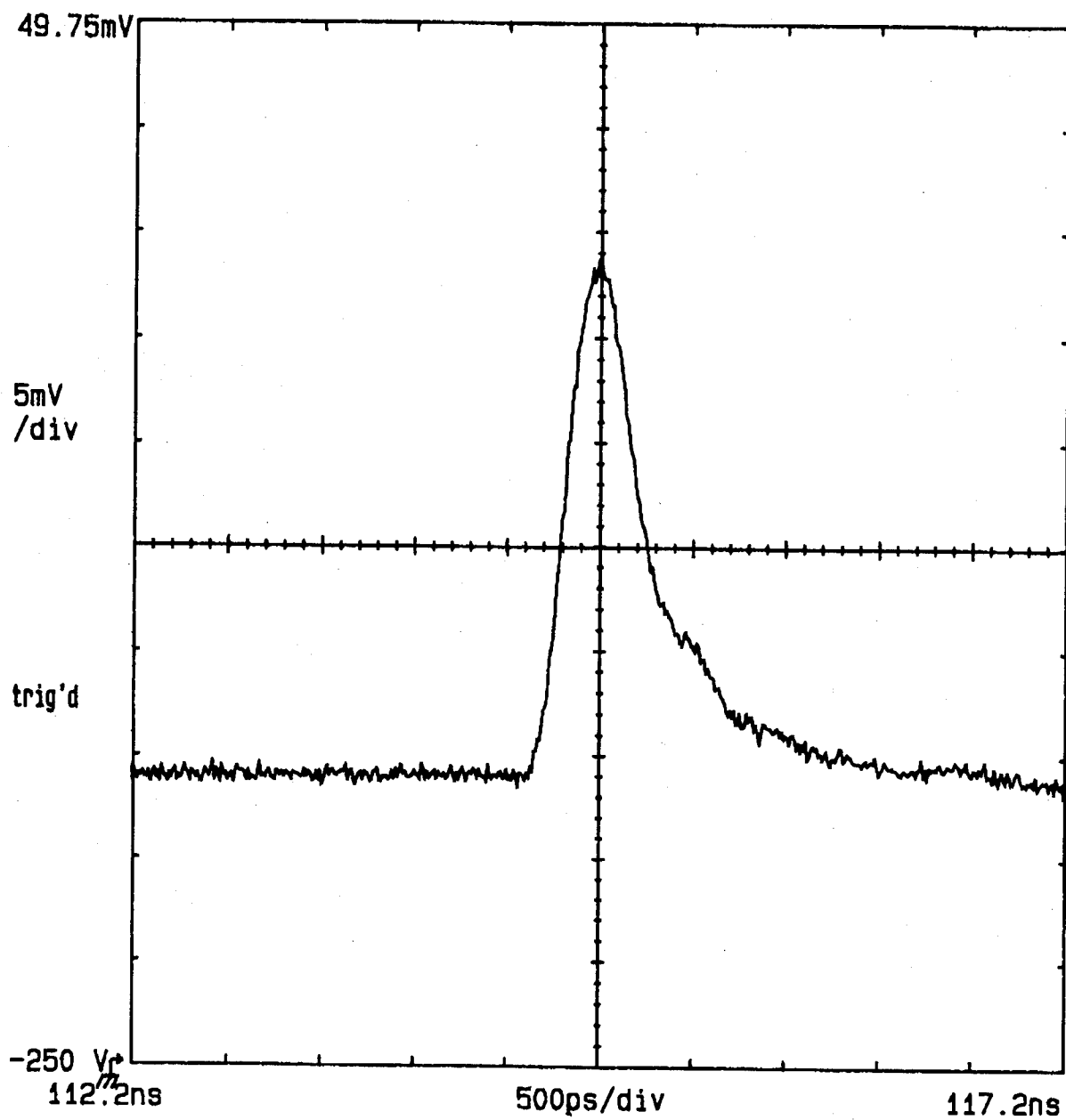


Figure 3.4 Electrical Pulse Width



Fi

Figure 3.5 Optical Pulse Prior to High Dispersion Fiber

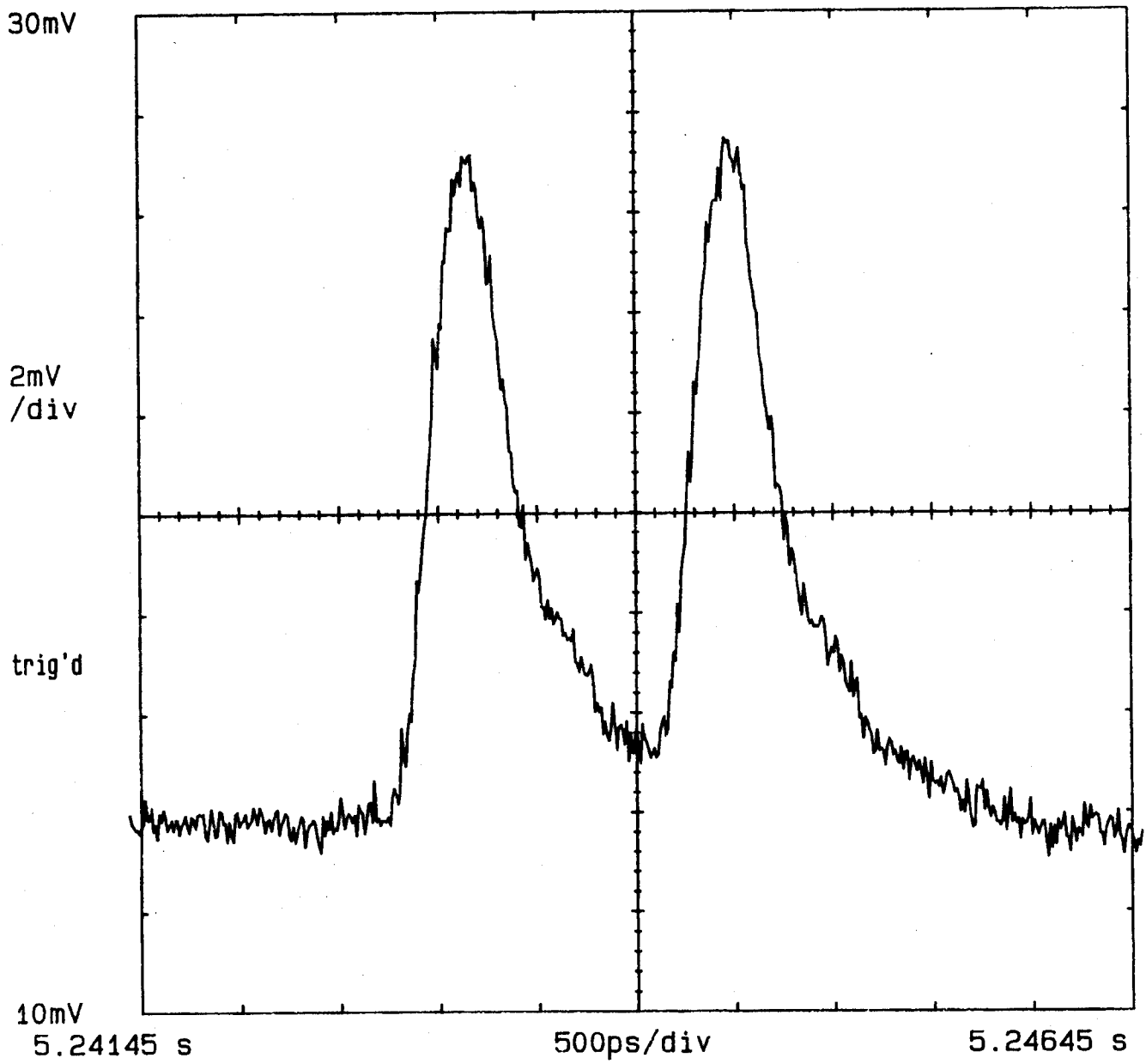
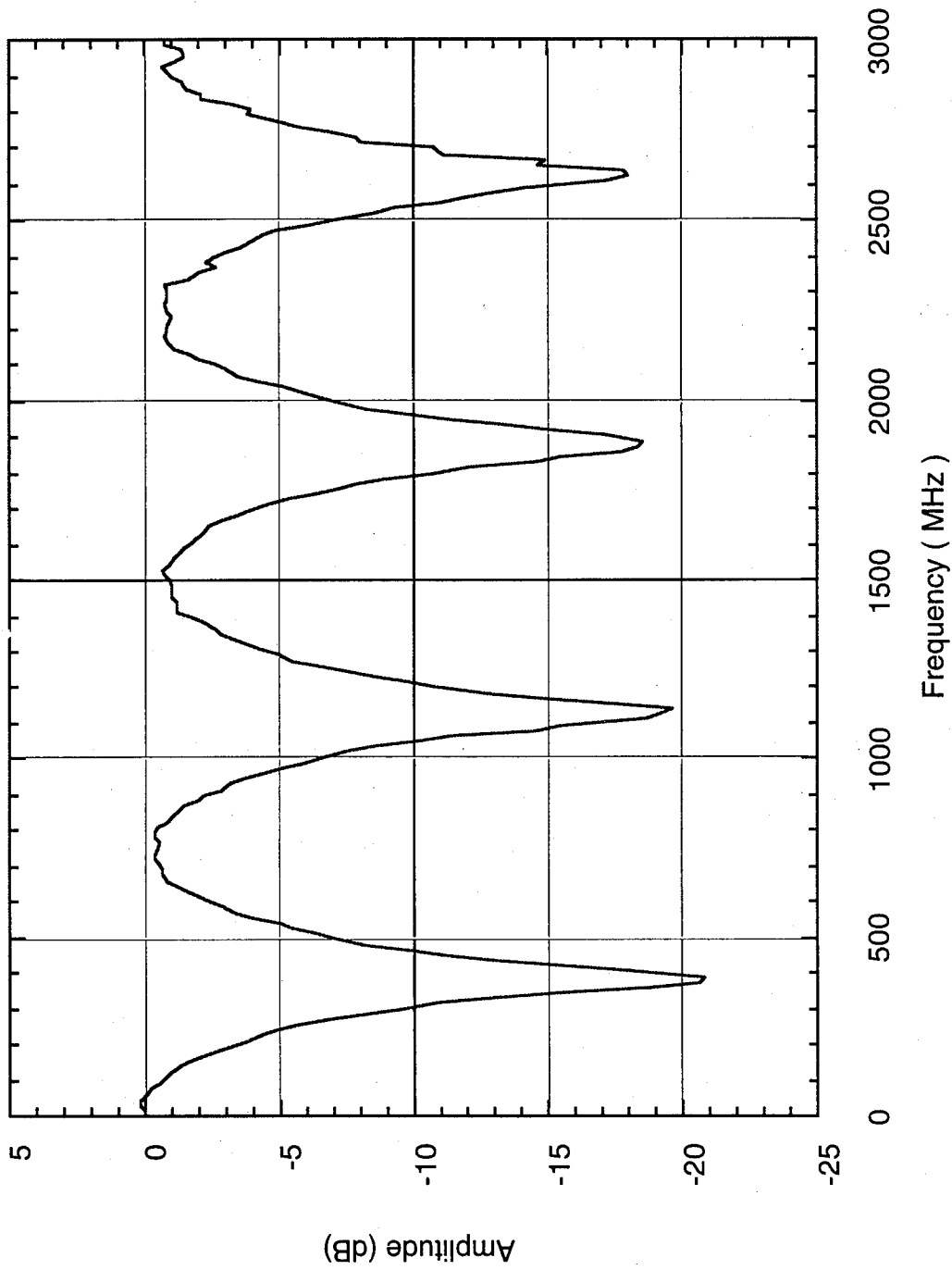
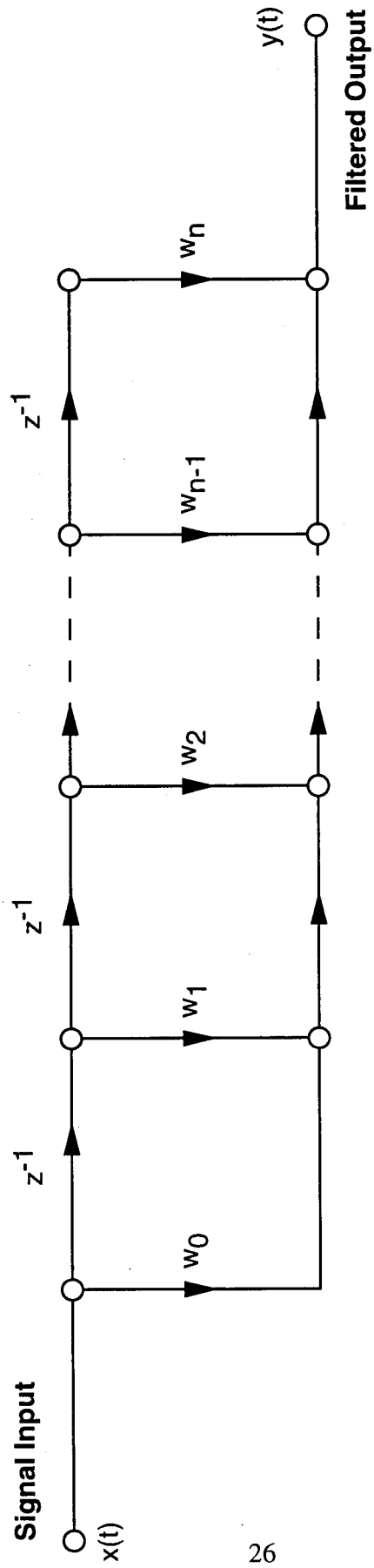


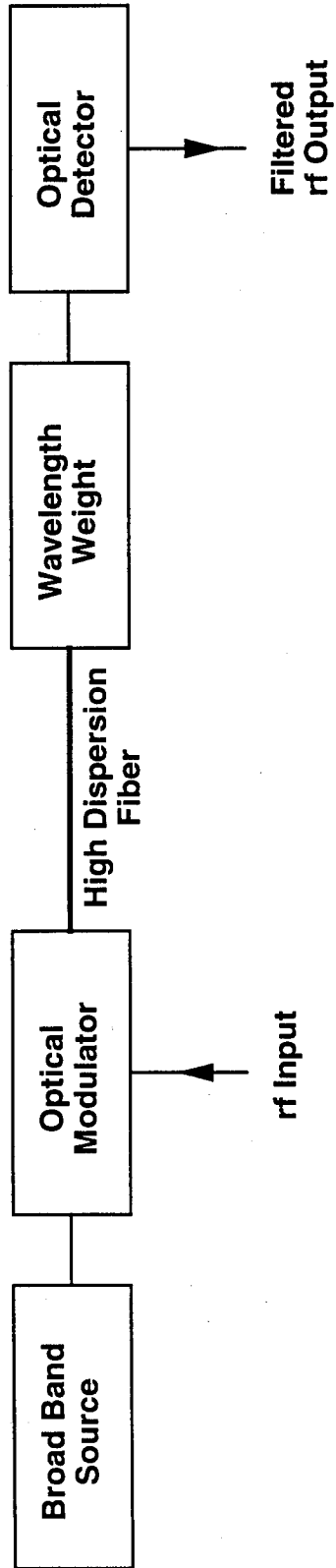
Figure 3.6 Impulse Response of Two Tap System



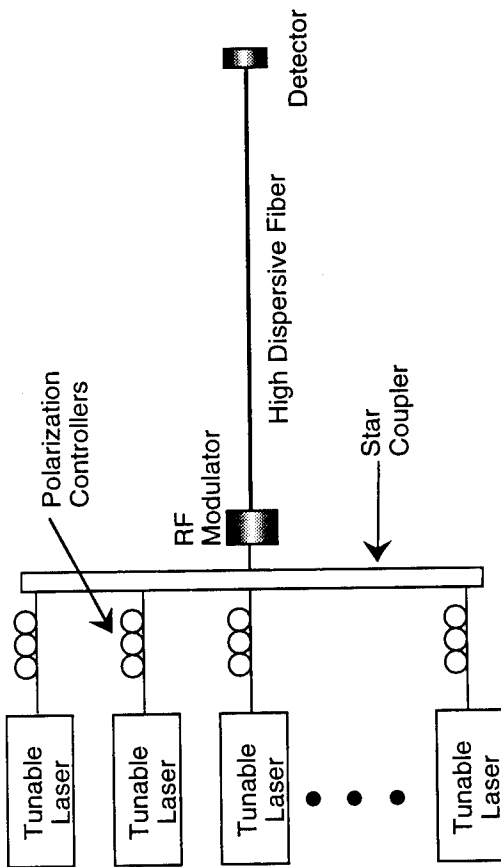
**Figure 3.7 Frequency Response of
Two Tap System**



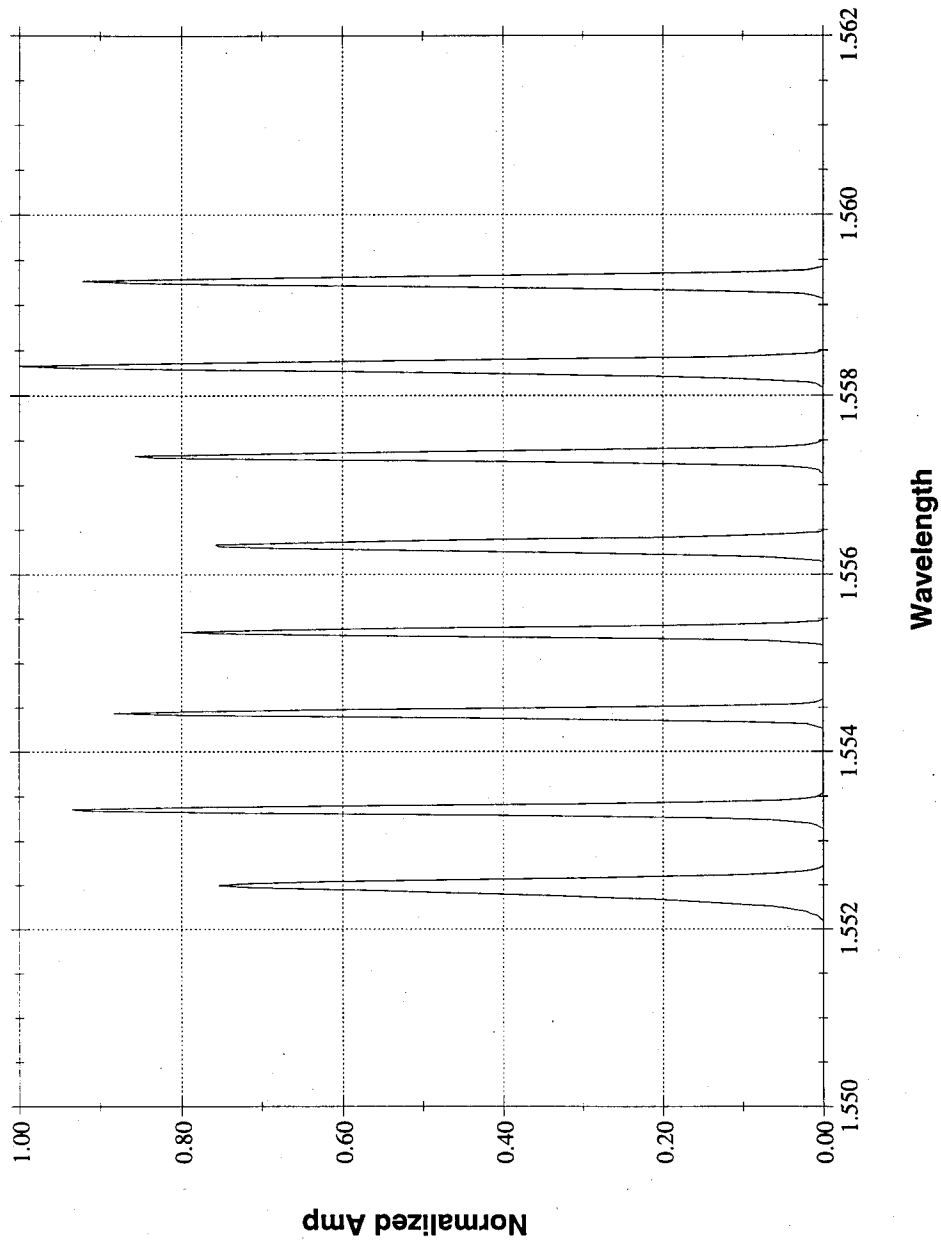
Transversal Filter
Figure 4.1



Idealized Optical Transversal Filter
Figure 4.2

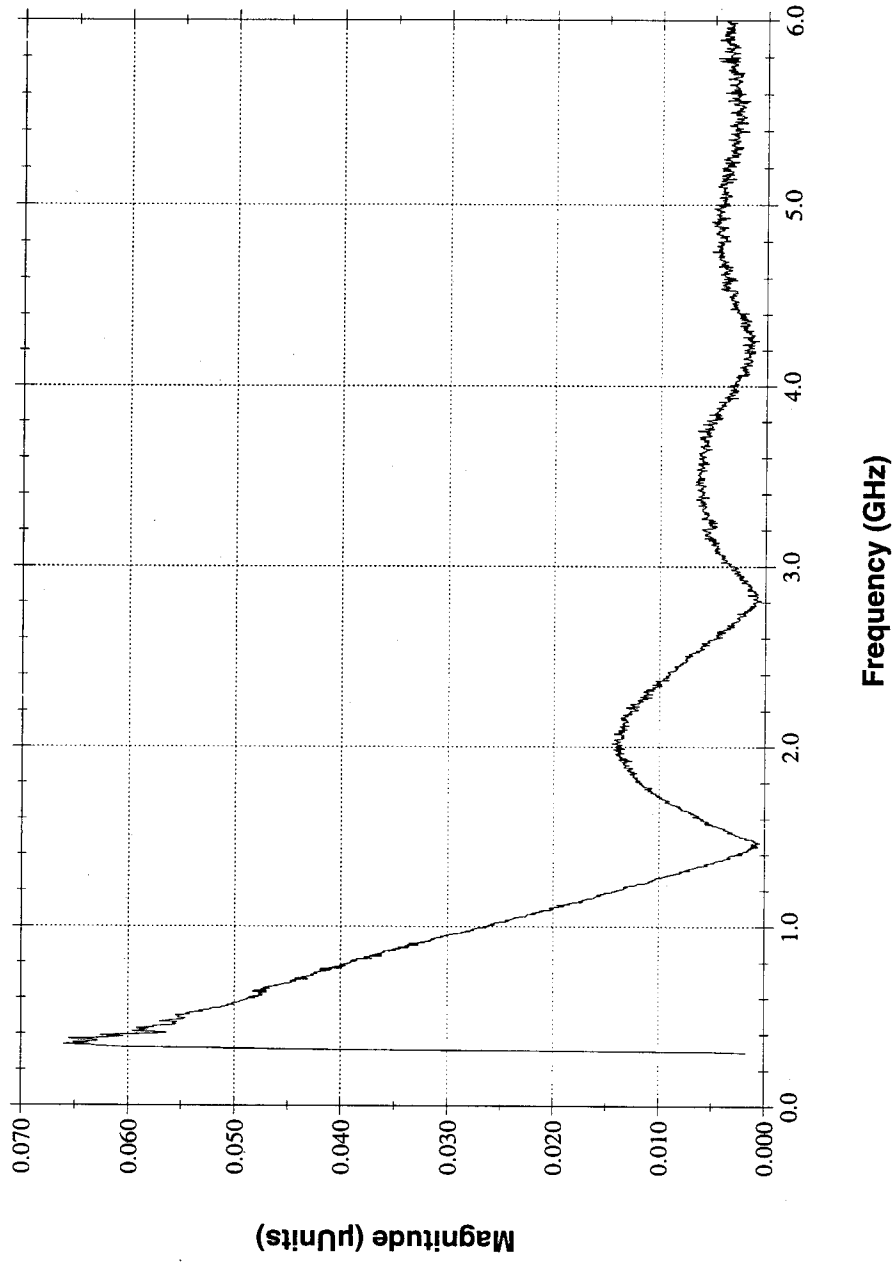


8 Channel Transversal Filter
Figure 4.3



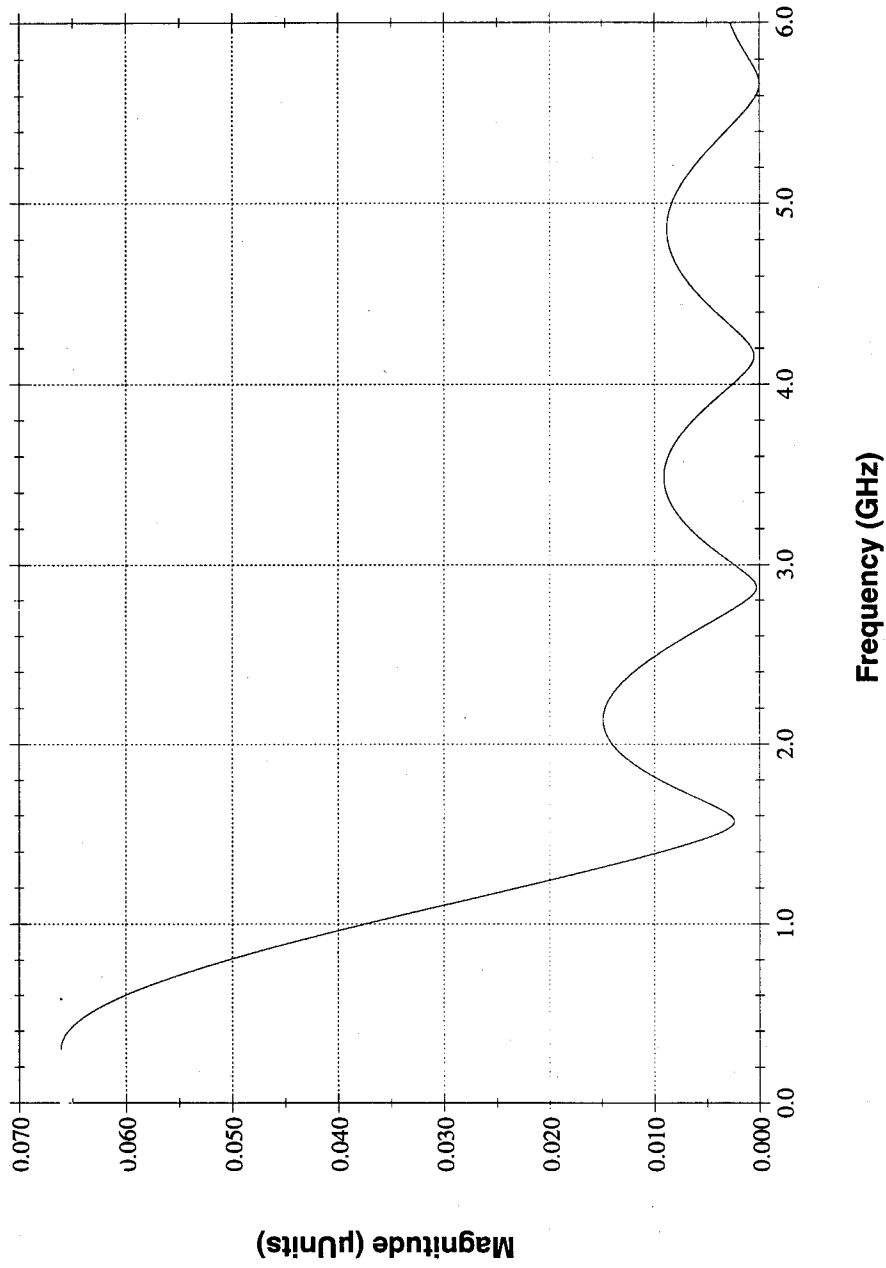
Laser Diode Spectrum with 0.87nm Wavelength Spacing

Figure 4.4



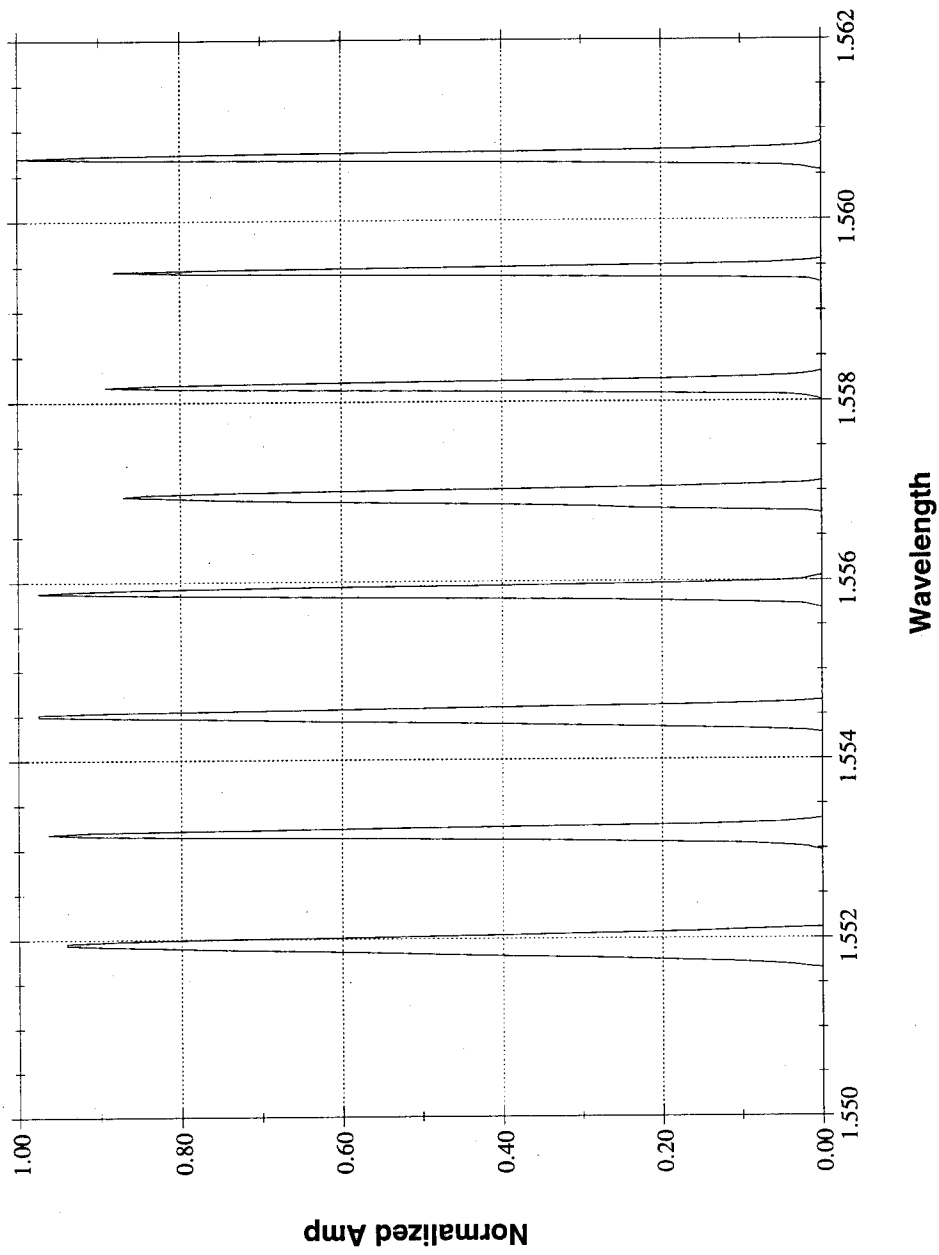
Measured Frequency Response for 0.87nm Wavelength Spacing

Figure 4.5



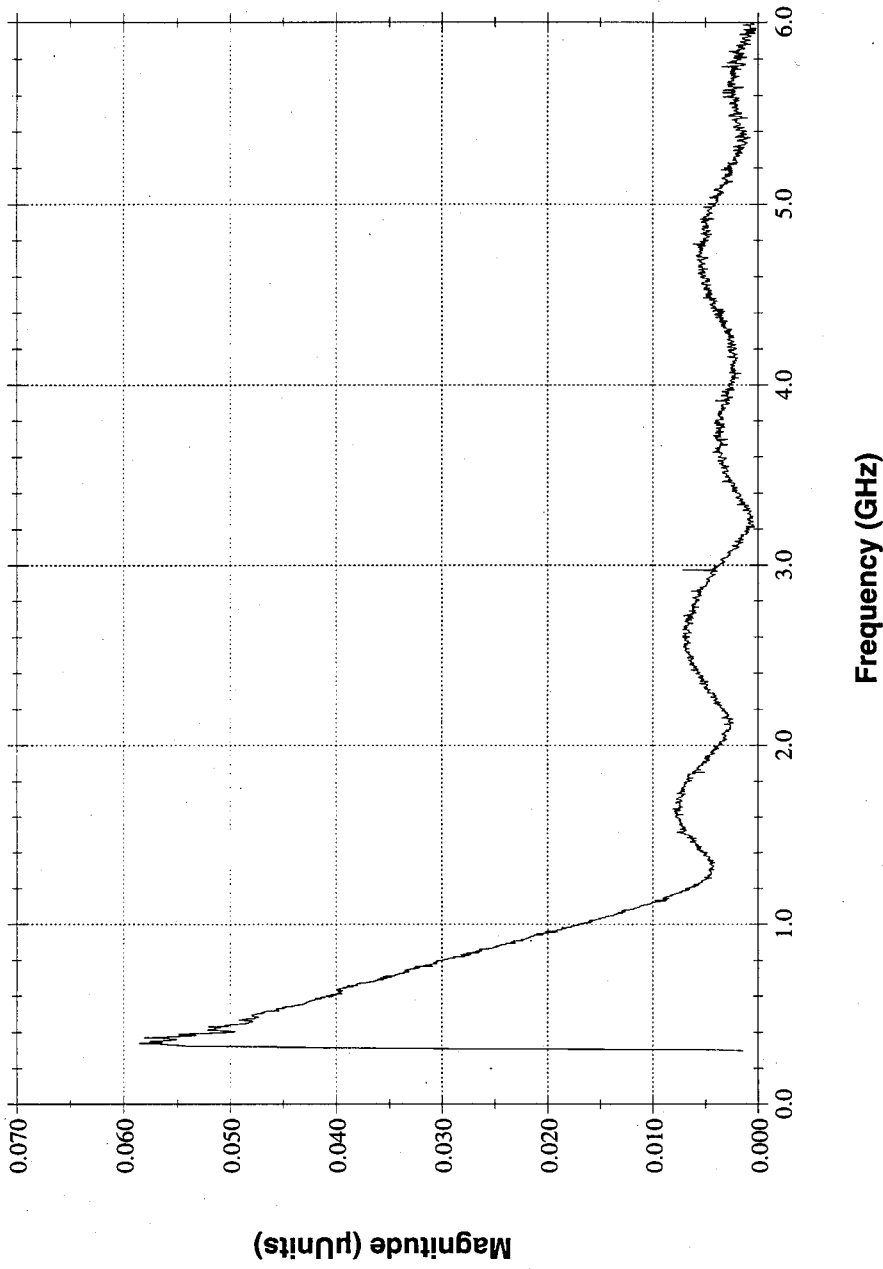
Calculated Frequency Response for 0.87nm Wavelength Spacing

Figure 4.6



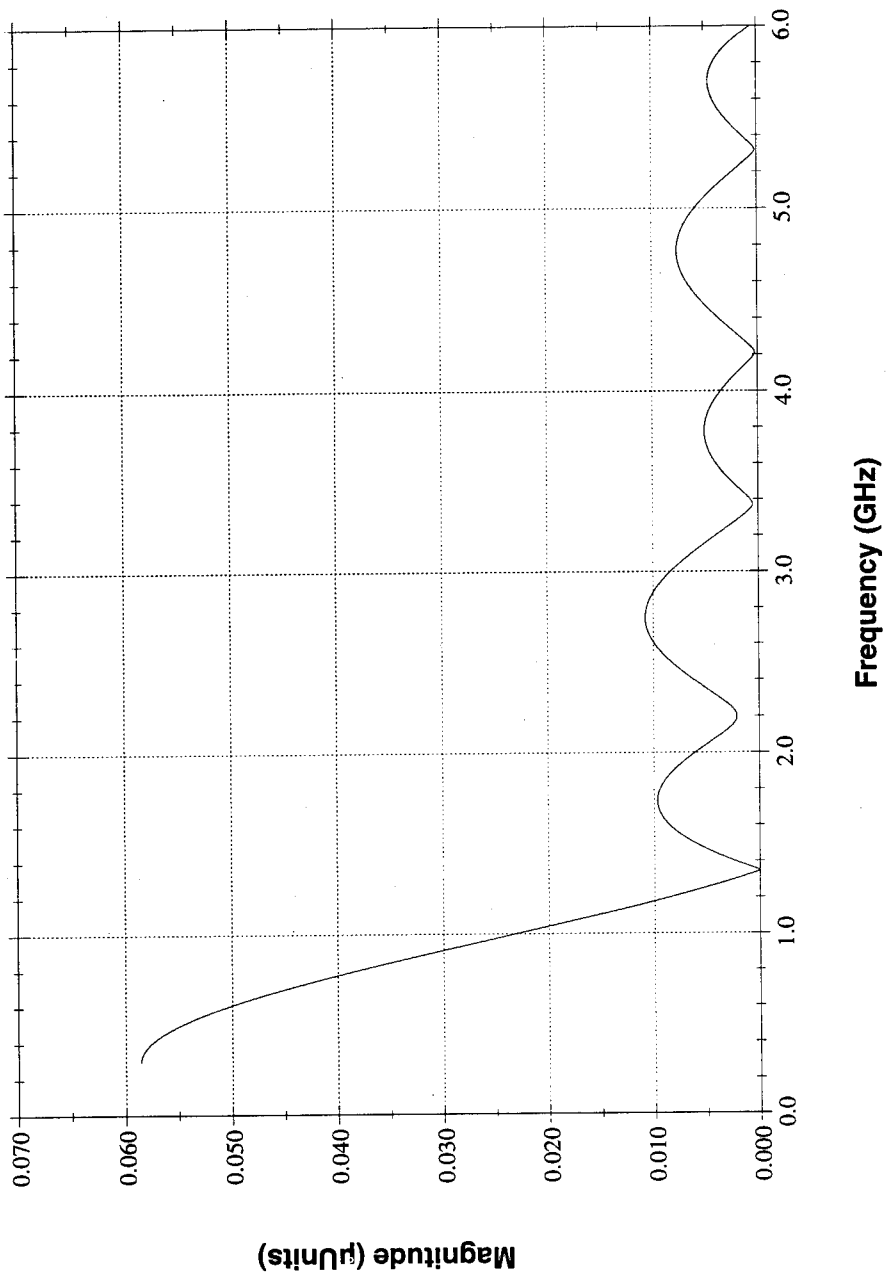
Laser Diode Spectrum with 1.24nm Wavelength Spacing

Figure 4.7



Measured Frequency Response for 1.24nm Wavelength Spacing

Figure 4.8



Calculated Frequency Response for 1.24nm Wavelength Spacing

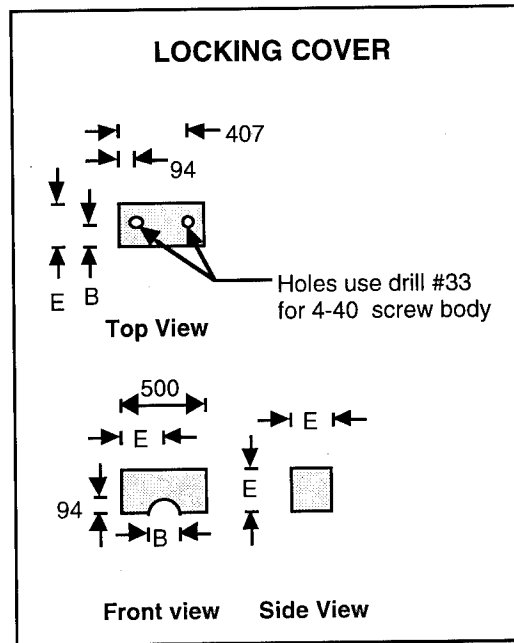
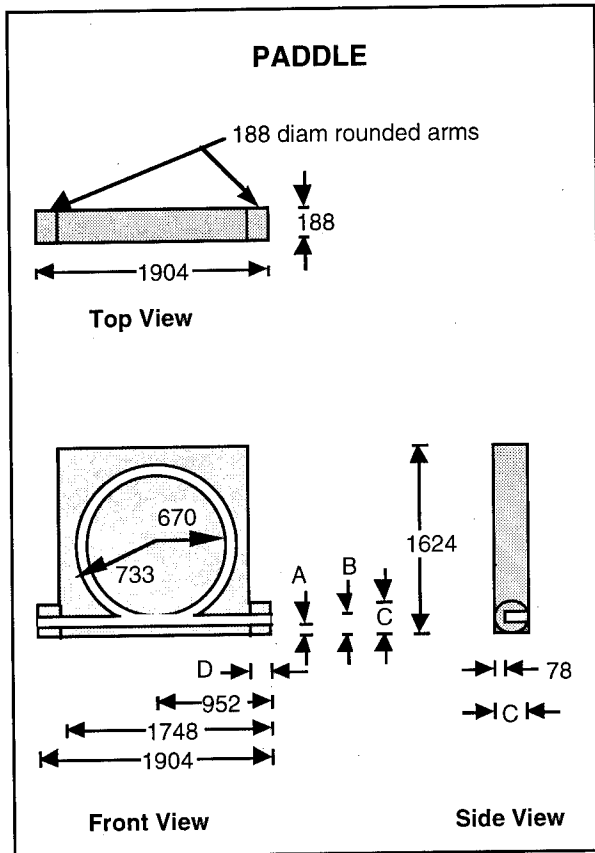
Figure 4.9

References

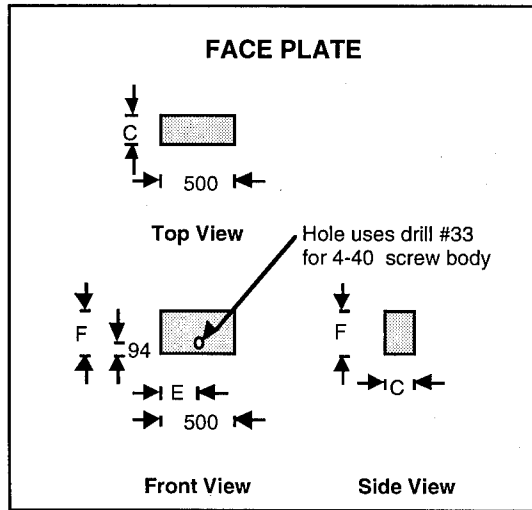
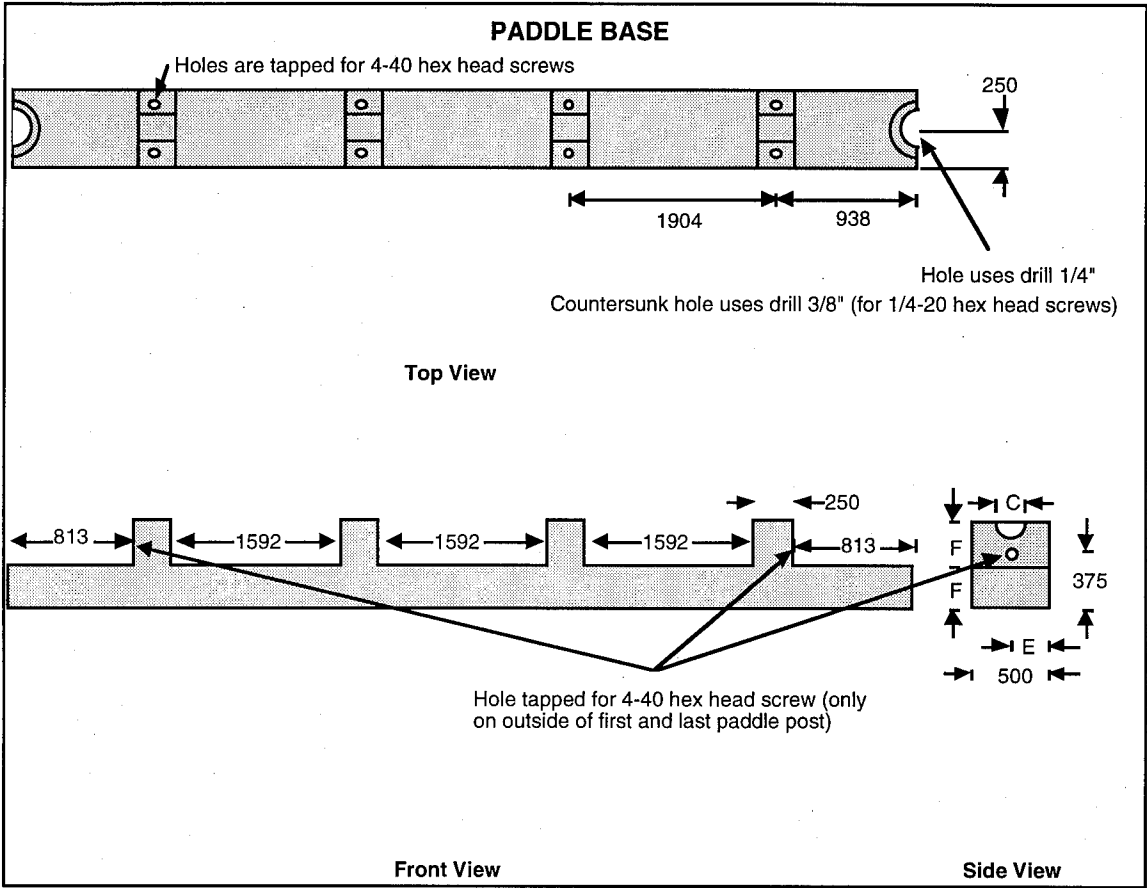
- 1 Seref, R.: "Optical Dispersion Technique for Time-Delay Beam Steering", Appl. Opt., 10 December 1992, pp. 7395-7397.
- 2 Soref, R.: "Wavelength Dependent, Tunable, Optical Time Delay System for Electrical Signals", U.S. Patent 9 June 1987, # 4671604.
- 3 Dugan, J.M., *et al.*: "All Optical, Fiber Based 1550 nm Dispersion Compensation in a 10Gbit/s, 150 km Transmission Experiment over 1310 nm Optimized Fiber", Conf. on Optical Fiber Comm., Postdeadline Paper, Digest, San Jose, Feb 1992, p. 367.
- 4 Favre, F., and Leguen, D.: "82 nm of Continuous Tunability for an External Cavity Semiconductor Laser", Electron. Lett., 1991, **27**, (2) pp. 183-184.
- 5 Alferness, R.C., *et al.*: "Broadly Tunable InGaAsP/InP Laser Based on a Vertical Couple Filter with 57 nm Tuning Range", Appl. Opt., 1992, **60**, (26), pp. 3209-3211.
- 6 Esman, R.D., *et al.*: "Microwave True Time-Delay Modulator Using Fiber Optic Dispersion", Electron. Lett., 1992, **20**, pp. 1905-1907.

Appendix A.

Design Of Polarization Controllers. (Units in 1/1000 of an inch)



- A = 63
- B = 125
- C = 188
- D = 156
- E = 250



- A = 63
- B = 125
- C = 188
- D = 156
- E = 250
- F = 281

Appendix B.

Mathematica Code to Calculate Filter Response

Calculates the filter created by the Delays and Weights entered below.

■ Load Fourier Package

```
<<Calculus`FourierTransform`;  
Context[FourierTransform];  
FourierFrequencyConstant=-1;
```

■ Set Pulse Width (line width of laser)

```
LineWidth = 0.025*10^-9;  
FiberLength = 1.0;  
Dispersion = 98*10^-3; ps / wavelength in meters;  
Dispersion2 = 101*10^-3; ps / wavelength in meters;  
Dispersion3 = 100*10^-3; ps / wavelength in meters;  
Dispersion4 = 98*10^-3; ps / wavelength in meters;  
Dispersion5 = 97*10^-3; ps / wavelength in meters;  
Dispersion6 = 95*10^-3; ps / wavelength in meters;  
Dispersion7 = 95*10^-3; ps / wavelength in meters;  
Dispersion8 = 96*10^-3; ps / wavelength in meters;  
PulseWidth = LineWidth * Dispersion;
```

■ Set Up Delays

```
Laser1 = 1.55196*10^-6;  
Laser2 = 1.55318*10^-6;  
Laser3 = 1.55451*10^-6;  
Laser4 = 1.55587*10^-6;  
Laser5 = 1.55697*10^-6;  
Laser6 = 1.55819*10^-6;  
Laser7 = 1.55942*10^-6;  
Laser8 = 1.56070*10^-6;  
  
Delay1 = 0;  
Delay2 = (Laser2-Laser1)*Dispersion2;  
Delay3 = (Laser3-Laser1)*Dispersion3;  
Delay4 = (Laser4-Laser1)*Dispersion4;  
Delay5 = (Laser5-Laser1)*Dispersion5;  
Delay6 = (Laser6-Laser1)*Dispersion6;  
Delay7 = (Laser7-Laser1)*Dispersion7;  
Delay8 = (Laser8-Laser1)*Dispersion8;
```

■ Set Weights

```
Amp1 = 0.94;  
Amp2 = 0.96;
```

```
Amp3 = 0.97;
Amp4 = 0.97;
Amp5 = 0.85;
Amp6 = 0.83;
Amp7 = 0.80;
Amp8 = 1.00;
```

■ Make Gaussian

```
Gaussian[t_,sigma_] := Exp[-(t^2)/(2 3.1415 sigma^2)];
```

■ Original Signal

```
signal[t_] = Gaussian[t,PulseWidth];
```

■ Delayed Version

```
delayedVersion[time_] = Amp1*signal[t-Delay1] +
Amp2*signal[t-Delay2] +
Amp3*signal[t-Delay3] +
Amp4*signal[t-Delay4] +
Amp5*signal[t-Delay5] +
Amp6*signal[t-Delay6] +
Amp7*signal[t-Delay7] +
Amp8*signal[t-Delay8];
```

■ Plot of Original and Delayed Version

```
sig = delayedVersion[t];
```

```
Plot[sig, {t, 0, Delay8}, GridLines -> None, PlotRange
-> All, Frame -> True]
```

■ Calculated the Spectrum of the Delayed Signal

```
FFTSig = FourierTransform[sig, t, w*2*3.1415];
```

```
Plot[Abs[FFTSig], {w, 0, 6*10^9}, GridLines -> None,
PlotRange -> All, Frame -> True, Ticks -> False]
```

```
sampled = Table[Abs[N[FFTSig]], {w, 3*10^6, 6*10^9,
3.7457838851*10^6}];
Put[CForm[sampled], "FFT"];
```

***MISSION
OF
ROME LABORATORY***

Mission. The mission of Rome Laboratory is to advance the science and technologies of command, control, communications and intelligence and to transition them into systems to meet customer needs. To achieve this, Rome Lab:

- a. Conducts vigorous research, development and test programs in all applicable technologies;
- b. Transitions technology to current and future systems to improve operational capability, readiness, and supportability;
- c. Provides a full range of technical support to Air Force Materiel Command product centers and other Air Force organizations;
- d. Promotes transfer of technology to the private sector;
- e. Maintains leading edge technological expertise in the areas of surveillance, communications, command and control, intelligence, reliability science, electro-magnetic technology, photonics, signal processing, and computational science.

The thrust areas of technical competence include: Surveillance, Communications, Command and Control, Intelligence, Signal Processing, Computer Science and Technology, Electromagnetic Technology, Photonics and Reliability Sciences.